

3D FACE RECOGNITION BASED ON EVOLUTION OF ISO-GEODESIC DISTANCE CURVES

Shun Miao, Hamid Krim

North Carolina State University
Electrical and Computer Engineering Dept.
Raleigh, NC 27606, USA

ABSTRACT

This paper presents a novel 3D face recognition method by means of the evolution of iso-geodesic distance curves. Specifically, the proposed method compares two neighboring iso-geodesic distance curves, and formalizes the evolution between them as a one-dimensional function, named evolution angle function, which is Euclidean invariant. The novelty of this paper consists in formalizing 3D face by an evolution angle functions, and in computing the distance between two faces by that of two functions. Experiments on Face Recognition Grand Challenge (FRGC) ver2.0 shows that our approach works very well on both neutral faces and non-neutral faces. By introducing a weight function, we also show a very promising result on non-neutral face database.

Index Terms— Face recognition, Geometric modeling, Image registration, Pattern classification

1. INTRODUCTION

Face recognition has been extensively researched over the last decade. Most of face recognition work is based on 2D images. In a controlled environment, current 2D face recognition techniques can achieve acceptable accuracy, but inadequate for more challenging applications, especially in the presence of variation of lighting conditions and pose [1]. The development of 3D scanning techniques provides a potential to alleviate impact of lightening and pose, and to therefore improve recognition performance.

Although more promising, the use of 3D images for face recognition also presents some challenges. First, as a surface in cartesian coordinates, a face is always subjected to Euclidean transform, and a face alignment stage is usually required before comparison, entailing additional computational cost. Second, in most scenarios, the 3D images we have are represented by random samples on the face, or triangulation without consistent parameterizations. As a result, 3D face comparison becomes a challenging task.

Iterative Cloud Point (ICP) algorithm [2] is widely used in face alignment, but it is time consuming and usually results in misalignment when two faces have different facial expressions. Recently, lots of studies have focused on feature points

on faces, and use them as landmarks to align and register them. Other approaches include [3], where 94 fiducial landmarks on 3D faces are extracted, three of which are used for alignment, prior to applying a Thin-Plate Spline warping to deform the surface. Another approach generates a face mesh from the 3D face point clouds, and uses manually picked feature points to subsequently apply a subdivision scheme for a consistent mesh. Xu et al. [4] developed a automatic subdivision technique for consistency of a mesh. Also there are other approaches for 2D imagery [5], which are focused on optical flow for yielding registration.

In this paper, we model the face geometry using the evolution of level set curves on a 3D surface. Using iso-geodesic distance curves, original point clouds are mapped into the same feature space, up to Euclidean transform. The indexing and arc length parameterizations provide a natural registration of 3D faces. The main contribution of this work is to propose a set of Euclidean invariant angle functions to represent the evolution of iso-geodesic distance curves. As a result, the problem of comparing surfaces can be solved by comparing two sets of one-dimensional function, and hence greatly simplified.

The reminder of the paper is organized as follows. In Section 2, we present details of the feature extraction algorithm, and show that it is Euclidean invariant. Matching distance based on extracted feature is proposed in Section 3. In section 4, we tested our method on FRGC Ver2.0 database [6], and the experiment shows very promising result. We close with conclusions and future work in Section 5.

2. METHOD DESCRIPTION

2.1. Face Detection and Preprocessing

The 3D images used in this paper are from the FRGC ver2.0 database, and are 640x480 face range images. At first, these raw images are down sampled by 4 in both X and Y direction. After down sampling, there are lots of techniques to detect a Region Of Interest (ROI) based on 2D images [7]. In this paper, we simply pick the point with the largest z-value as the rough location of the nose tip, and select all vertices with a distance to nose tip less than 100mm as ROI.

Upon identifying a ROI, a Delaunay triangulation is applied to (x,y) component of vertices to generate a triangular mesh. Most 3D scanners will introduce holes around the eye and eyebrow region, and a Delaunay triangulation will automatically fill the holds by large triangles. Geodesic distances are computed on the basis of the triangulated mesh, and a greater precision is achieved by smoothing the effect of noise.

2.2. Iso Geodesic Distance Curves

The idea of using iso-geodesic distance curves (Iso-curves) as features for face recognition was first proposed by Shuo *et al.* in [8]. A practical method of extracting iso-curves was also introduced in [8].

A geodesic distance between two points on a manifold is defined as the arc length of the shortest path between these two points on the manifold. If we choose a face M to be the manifold, the geodesic distance between a point p and nose tip is defined as the Geodesic Distance Function (GDF) at p_0 . As such, iso-curves with level c may be defined as:

$$P^c = \{p | g_M(p) = c, p \in M, \}$$

Where M is a face range surface in R^3 , and $g_M(\cdot)$ is a GDF on M .

To compute iso-curves, at first, a fast marching algorithm, introduced by J.Sethian [9] is applied to compute geodesic distances. A geodesic distance computed by the fast marching algorithm is the real shortest path on a triangulated surface, and is consistent with the real geodesic distance. Iso-curves are then extracted at a level $c_i = i \cdot \Delta c, i = 1, 2, 3 \dots 40$, where $\Delta c = 2$ (all units in this paper are in millimeters)

As illustrated in [8], an open mouth is a practical problem because it introduces a hole on the surface, changing the topology of both the surface and some associated the Iso-curves. We adopt a method to eliminate the mouth region from every face surface to preserve a uniform topology across faces.

2.2.1. Curve Parameterizations

The absence of the mouth regions from faces, unfortunately yields an inconsistent topology of the iso-curves, some of which are open and others closed. To compare curves with different topologies, we need a consistent parameterization which will be unaffected by topological change. In this paper, we choose a slightly modified arc length parameterization.

First, a symmetric plane can be easily detected [10], and each iso-curve is divided into two parts. These two parts are then independently parameterized by arc length, with the starting points at the top, denoted as $P_{left}(l)$ and $P_{right}(l)$. The parameterization of the whole curve is: (see Fig.1 for example)

$$P(l) = \begin{cases} P_{left}(-l), & l < 0 \\ P_{right}(l), & \text{o.w.} \end{cases}$$

In practice, iso-curves are of course discrete:

$$P[k] = P(k\Delta l), \quad k = [a, b], \quad \Delta l = 2$$

Where $[a, b]$ is the range of arc length parameterizations. Because of the diversity of arc length of iso-curves, ranges are usually different for different images. In this paper, we focused on the common range shared by all images.

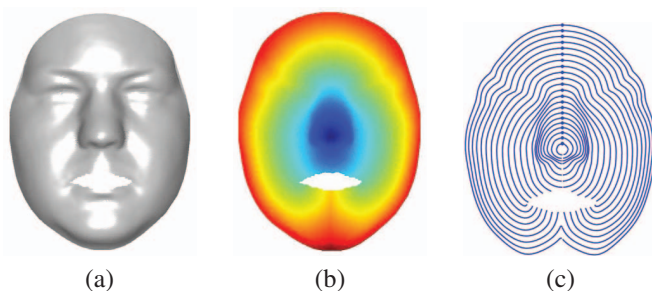


Fig. 1. (a) Smoothed 3D face (b) Color-coded Geodesic Distance Function (c) Iso-curves, starting point is marked on each curve. To be clear, only iso-curve with even index are displayed

2.3. Euclidean Invariant Evolution Angle Function

In this section, a vector function is developed to describe the evolution from the i^{th} iso-curve to the $(i+1)^{st}$, by specifying the direction to which each point on the i^{th} iso-curve is moving. To avoid variations due to the Euclidean group transform, a moving frame is generated on each iso-curve, and the vector function is represented by a simple angle function. This is clearly Euclidean invariant, and will be used as feature for our classifier.

2.3.1. Evolution Vector Function

Consider the tangent plane at a point of a c -level iso-curve, denoted as T_p . We can define two orthogonal vectors to span this tangent plane, one being the tangent vector of the iso-curve at a point p , denoted as $t(p)$, and the other being orthogonal to $t(p)$, denoted as $v(p)$. For a point $\tilde{p} = p + \varepsilon \cdot v(p)$, the closest point on P^c is p , so the GDF of \tilde{p} is (see Fig.2 for example):

$$f(p + \varepsilon \cdot v(p)) = f(p) + \varepsilon.$$

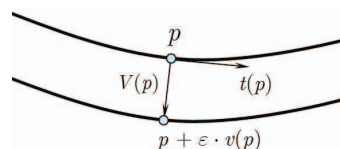


Fig. 2. Illustration of evolution of iso-curves.

With this property of the GDF, if we choose a level to c_i , and ε to be Δc , which is assumed sufficiently small, at any point on the i^{th} iso-curve, we have,

$$\forall p \in P^i, p + \Delta c \cdot v(p) \in P^{i+1}$$

$$v(p) \perp t(p)$$

The vector $v(p)$ is called a unit evolution vector, and the evolution vectors are parameterized by the arc length any iso-curve, it becomes a function of arc length, and becomes a *unit evolution vector function* $v^i(l)$. Correspondingly, $\Delta c \cdot v^i(l)$ is an evolution vector function. The evolution between iso-curves is explicitly described by an evolution vector function, and the evolution can be written as Eq. (1). Note that the $(i + 1)^{st}$ iso-curve may have a different parameter L because evolution cannot guarantee the preservation of the arc length parameterization.

$$P^{i+1}(L) = P^i(l) + \Delta c \cdot v^i(l) \quad (1)$$

2.3.2. Evolution Angle Function

While the evolution vector function includes all the information required to reconstruct a surface, it is not a complete shape descriptor for pattern recognition, as it is subject to Euclidean transform variability, and the precise face alignment this entails, is often a challenging task. To that end, we opt for a local description by way of a moving frame along an iso-curve, and where an evolution vector can be explicitly written as an angle.

It is shown that unit evolution vector $v(p)$ is perpendicular to the unit tangent vector $t(p)$. Thus, if we are given a reference vector in the perpendicular plane, $v(p)$ can be determined by an angle to the reference vector, which is Euclidean invariant. To generate a set of reference vectors along an iso-curve, we establish a moving frame $\{r^i(l), s^i(l), t^i(l)\}$ along it. $t^i(l)$ is the unit tangent vector which can be computed by the curve itself. Vectors from the nose tip to the iso-curve are denoted as $x^i(l)$, and the other two vectors are defined as:

$$r^i(l) = \frac{x^i(l) - x^i(l) \cdot t^i(l)}{\|x^i(l) - x^i(l) \cdot t^i(l)\|}$$

$$s^i(l) = r^i(l) \times t^i(l).$$

The unit evolution function can then be written as a function of angle $\theta^i(l)$, and will be referred to as the *evolution angle function* (EAF):

$$v^i(l) = r^i(l) \cos(\theta^i(l)) + s^i(l) \sin(\theta^i(l)) \quad (2)$$

By substituting Eq. (2) to Eq. (1), the evolution between two neighboring iso-curves is explicitly determined by EAF. As a result, the comparison problem between two faces is equivalent to that of comparing EAFs. This is a much simpler task as we avoid the surface alignment and registration problem. A set of evolution angle functions is shown in Fig. 3.

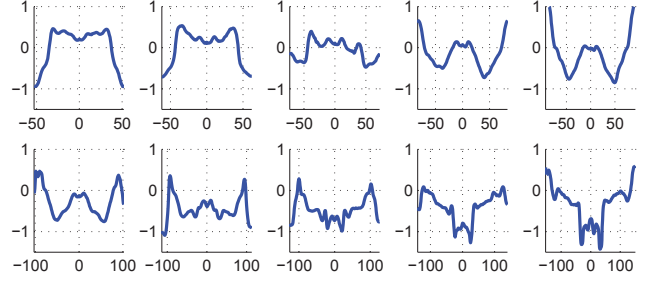


Fig. 3. Examples of Evolution Angle Functions

3. RECOGNITION

Because of facial expressions, faces are subjected to non-rigid transformations, and some sections of the of iso-curves are also subjected to these non-rigid transformation, with the most pronounced around the mouth and cheek regions. An invariance to a Euclidean transform is hence insufficient, and for robustness to non-rigid transforms, we analyze class separability of these curves. A robust part of each iso-curve is identified and selected as the feature for classification.

In our experiments, EAF is a discrete function, represented by samples $\theta^i[k]$. For the advantage of computational simplicity, we individually treat each sample on EAF. In training data, there are 30 subjects, and 4 3D scans for each face. EAF of the m^{th} scan of the n^{th} subject is denoted as $\{\theta_{m,n}^i[k]\}$. The separability confidence in [11] is adopted:

$$C^i[k] = \frac{N \cdot \sum_{m=1}^M (\bar{\theta}_m^i[k] - \bar{\theta}^i[k])^2}{\sum_{n=1}^N \sum_{m=1}^M (\theta_{m,n}^i[k] - \bar{\theta}_m^i[k])^2}$$

where

$$\bar{\theta}_m^i[k] = \frac{1}{N} \sum_{n=1}^N \theta_{m,n}^i[k], \quad \bar{\theta}^i[k] = \frac{1}{MN} \sum_{n=1}^N \sum_{m=1}^M \theta_{m,n}^i[k].$$

The numerator is the summation of variance of $\theta^i[k]$ over each subject, and the denominator is the variance of $\theta^i[k]$ over the whole training data. The larger $C^i[k]$ is, the better separability $\theta^i[k]$ has. Using this confidence, a weighting function is defined as Eq.3, to describe a thresholding criterion $C^i[k]$, and to only select the feature with $C^i[k] \geq \gamma$

$$w^i[k] = \begin{cases} 0, & \text{for } C^i[k] < \gamma \\ 1, & \text{for } C^i[k] \geq \gamma \end{cases} \quad (3)$$

With weighting function, the matching distance between two EAFs, $\theta^i[k]$ and $\tilde{\theta}^i[k]$, is defined as Eq.4:

$$D(\theta, \tilde{\theta}) = \sum_{i=1}^{40} \sum_{k=a_i}^{b_i} [(\theta^i[k] - \tilde{\theta}^i[k]) \cdot w^i[k]]^2 \quad (4)$$

Where, $[a_i, b_i]$ is the range of i^{th} iso-curve. We will show the Receiver Operation Characteristic (ROC) curve and matching accuracy based on this matching distance.

4. EXPERIMENTS AND RESULTS

We collected 30 subjects as a training set from Face Recognition Grand Challenge II (FRGC2) Spring 2004 database. In the training set, each subject provides 4 different expressions. Our experiment is performed on 200 images of 50 subjects. For each subject, we collected two neutral images and two non-neutral images (including smile, surprise, inflated and frown). First, 50 neutral faces are selected as gallery templates, and 150 independent 3D scans for testing. The rank1 and rank2 recognition rate based on the matching distance is provided in table.1. The matching distance between every pair of images (19900 in total) is computed to generate Receiver Operation Characteristic (ROC) Curve, which is shown in Fig. 4.

Table 1. Rank1 and Rank2 recognition rate

	Neutral faces	Non-neutral faces
Rank1	100%	93.64%
Rank2	100%	95.46%

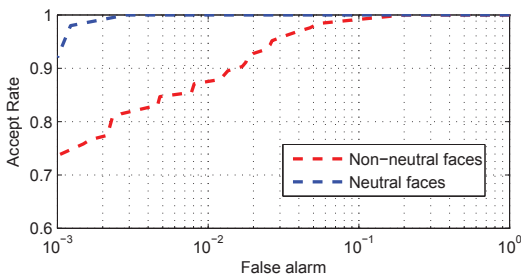


Fig. 4. ROC curves for experiment on FRGC ver.2.0 database.

5. CONCLUSION AND FUTURE WORKS

We present a 3D face recognition by formalizing the evolution of iso-curves as $[0, 2\pi]$ valued one-dimensional evolution angle function, which is used as feature for classifier, and is shown to be Euclidean invariant. For robustness to facial expressions, we analyze class separability to select a robust part of each iso-curve, and define the matching distance based on them. The promising recognition rate using the proposed method demonstrates the efficiency of using EAF for 3D face recognition. Possible future work includes picking other points rather than nose tip as reference point to generate iso-curves, and investigating their effectiveness.

6. REFERENCES

- [1] Kevin W. Bowyer, Kyong Chang, and Patrick Flynn, “A survey of approaches and challenges in 3d and multi-modal 3d face recognition,” *Computer Vision and Image Understanding*, vol. 101, no. 1, pp. 1 – 15, Dec. 2006.
- [2] Zhengyou Zhang, “Iterative point matching for registration of free-form curves and surfaces,” *International Journal of Computer Vision*, vol. 13, no. 2, pp. 119 – 52, 1994.
- [3] Xiaoguang Lu and A.K. Jain, “Deformation modeling for robust 3d face matching,” *Pattern Analysis and Machine Intelligence, IEEE Transactions on*, vol. 30, no. 8, pp. 1346–1357, Aug. 2008.
- [4] Chenghua Xu, Yunhong Wang, Tieniu Tan, and Long Quan, “Automatic 3d face recognition combining global geometric features with local shape variation information,” Los Alamitos, CA, USA, 2004, pp. 308 – 13.
- [5] V. Blanz and T. Vetter, “Face recognition based on fitting a 3d morphable model,” *Pattern Analysis and Machine Intelligence, IEEE Transactions on*, vol. 25, no. 9, pp. 1063–1074, Sept. 2003.
- [6] P.J. Phillips, P.J. Flynn, T. Scruggs, K.W. Bowyer, Jin Chang, K. Hoffman, J. Marques, Jaesik Min, and W. Worek, “Overview of the face recognition grand challenge,” in *Computer Vision and Pattern Recognition, 2005. CVPR 2005. IEEE Computer Society Conference on*, June 2005, vol. 1, pp. 947–954 vol. 1.
- [7] Erik Hjelmas and Boon Kee Low, “Face detection: A survey,” *Computer Vision and Image Understanding*, vol. 83, no. 3, pp. 236 – 274, 2001.
- [8] S. Feng, H. Krim, and I. A. Kogan, “3d face recognition using euclidean integral invariants signature,” in *Statistical Signal Processing, 2007. SSP '07. IEEE/SP 14th Workshop on*, Aug. 2007, pp. 156–160.
- [9] J. A. Sethian, “A fast marching level set method for monotonically advancing fronts,” *Proceedings of the National Academy of Sciences of the United States of America*, vol. 93, no. 4, pp. 1591 – 1591, 1996.
- [10] Y. Wang, X. Tang, J. Liu, G. Pan, and R. Xiao, “3d face recognition by local shape difference boosting,” in *European Conference on Computer Vision*, 2008.
- [11] Xiaoxing Li, Tao Jia, and Hao Zhang, “Expression-insensitive 3d face recognition using sparse representation,” in *Computer Vision and Pattern Recognition Workshops, 2009. CVPR Workshops 2009. IEEE Computer Society Conference on*, June 2009, pp. 2575–2582.